

A global study of 2D dissipative diffeomorphisms with a homoclinic figure-eight

Carles Simó

Dept. Matemàtica Aplicada i Anàlisi, UB

`carles@maia.ub.es`

Joint work with S. Gonchenko and A. Vieiro

From Dynamics to Complexity

Celebrating the work of Mike Shub

Fields Institute, U. of Toronto

Toronto

1205101710

Contents

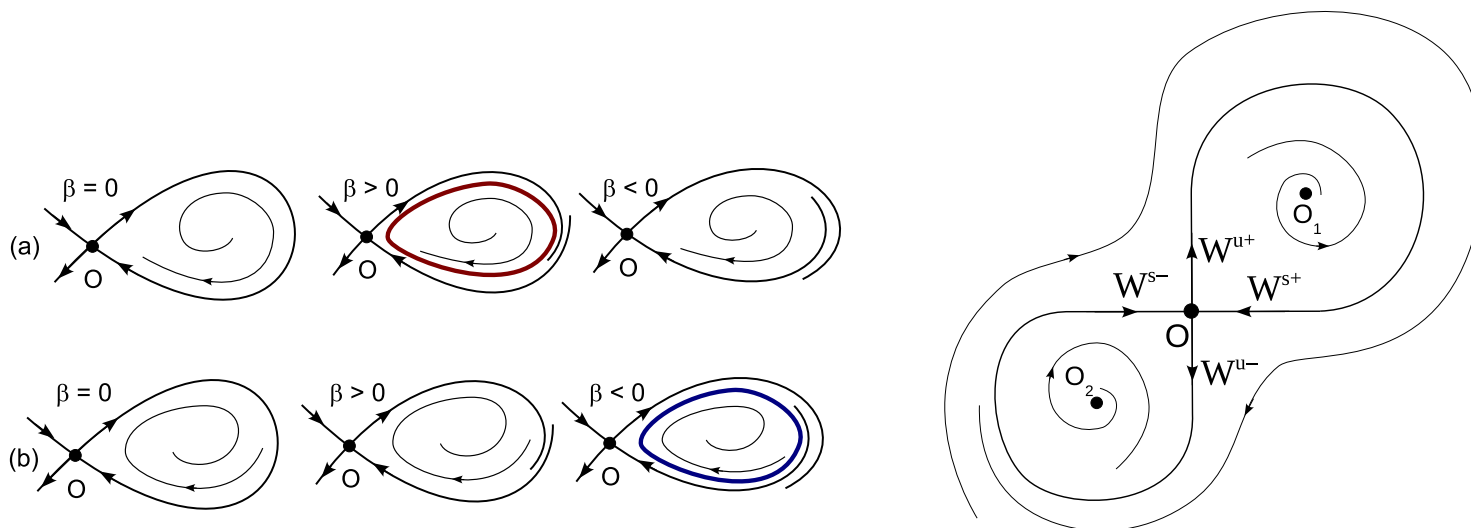
- Motivation
- The flow case: the bifurcation diagram
- The diffeomorphism case: the bifurcation diagram
- Different kinds of strange attractors
- A dissipative figure-eight separatrix model. Ranges
- A preliminary exploration
- Kinds of tangencies and some homoclinic intersections
- Bifurcation structure in the $\mathbb{H}\mathbb{Z}^{\pm, \mp}$ domains
- Some theoretical results
- Further exploration of the model: global views
- Domains of sinks, Lyapunov exponents, some attractors
- A sample of tools: cubic returns, sinks approaching a s-n
- An illustration of blowing up near the limit
- Outlook: open problems and extensions

Motivation

Consider a **pendulum like system** under **forcing and dissipation**. **Forcing**: elliptic point \rightarrow a repellor. **Dissipation**: move the dynamics towards the separatrix. Eigenvalues at the saddle: $\gamma, -\lambda$ with $0 < \gamma < \lambda$. The usual **cylinder-sphere-stereo projection** allows to have a **dissipative figure-eight**.

Compare left plot (unfolding a dissipative loop) to the right one: figure-eight before unfolding.

Next plot shows the **bifurcation diagram for flows**.



The flow case: the bifurcation diagram

Let μ_1, μ_2 be splitting parameters.

Theorem:

Six regions appear in the **Turaev bifurcation diagram**. The boundaries correspond to:

$$W^{u+} = W^{s+} \quad (\text{I} \rightarrow \text{II});$$

$$W^{u-} = W^{s+} \quad (\text{II} \rightarrow \text{III});$$

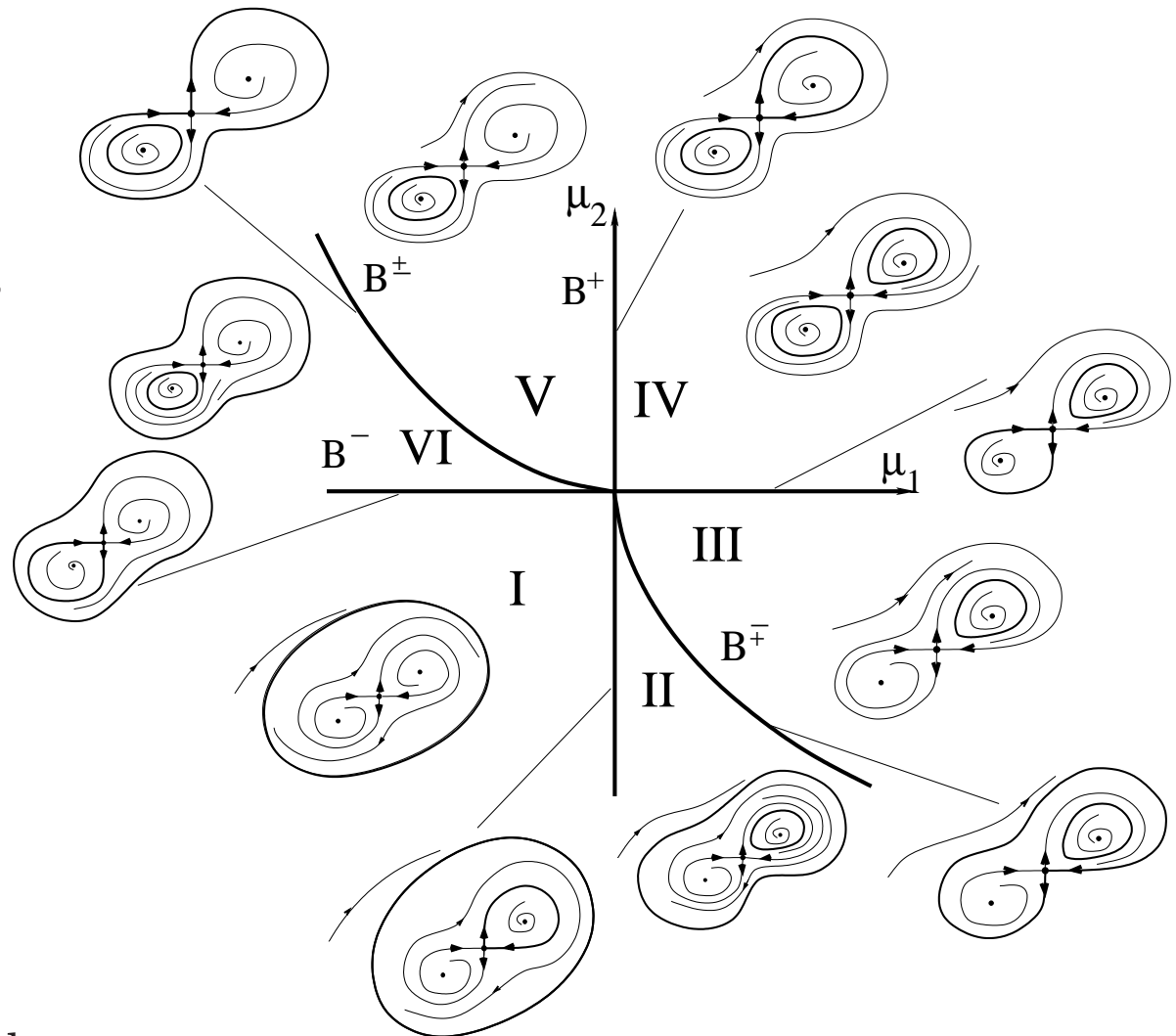
$$W^{u-} = W^{s-} \quad (\text{III} \rightarrow \text{IV});$$

$$W^{u+} = W^{s+} \quad (\text{IV} \rightarrow \text{V});$$

$$W^{u+} = W^{s-} \quad (\text{V} \rightarrow \text{VI});$$

$$W^{u-} = W^{s-} \quad (\text{VI} \rightarrow \text{I});$$

The ones with same connection differ on the behavior of the other branch.



If every line splits in 2 (first-last tangency) we shall have 17 regions.

Different kinds of strange attractors

A priori we can consider that different kinds of attractors will show up:

- Attractors which appear after a **period doubling cascade** of sinks. They have a **local** character.
- The ones in region **19** or **global attractors** when all the manifolds intersect.
- Attractors in regions **18, 26** or **tail attractors** with partial intersections of manifolds.
- The ones obtained by **folding** of the invariant curves around O_1 or O_2 , which appear when the invariant curve becomes **tangent to the stable foliation** of the saddle.
- Attractors obtained by **folding** of the invariant curves around both O_1 and O_2 , with the same mechanism.

A dissipative figure-eight separatrix model. Ranges

We introduce the following model

$$M_{a,b,\psi,A,\omega} : \begin{pmatrix} z \\ \eta \\ s \end{pmatrix} \mapsto \begin{pmatrix} z + \omega_j + A \log(|y|) \\ \text{sign}(y)|y|^\psi \\ \text{sign}(y)s \end{pmatrix},$$

where $y = a_j + \eta + b_j \sin(2\pi z)$ and the index j takes the value 1 if $s = 1$ and the value 2 if $s = -1$. η (resp. y) position wrt unstable (resp. stable) manifolds. Positive pointing to the saddle.

It can be seen as a generalization of the **separatrix map** (Chirikov et al.) and also of the **fattened Arnold map** (Broer,S,Tatjer).

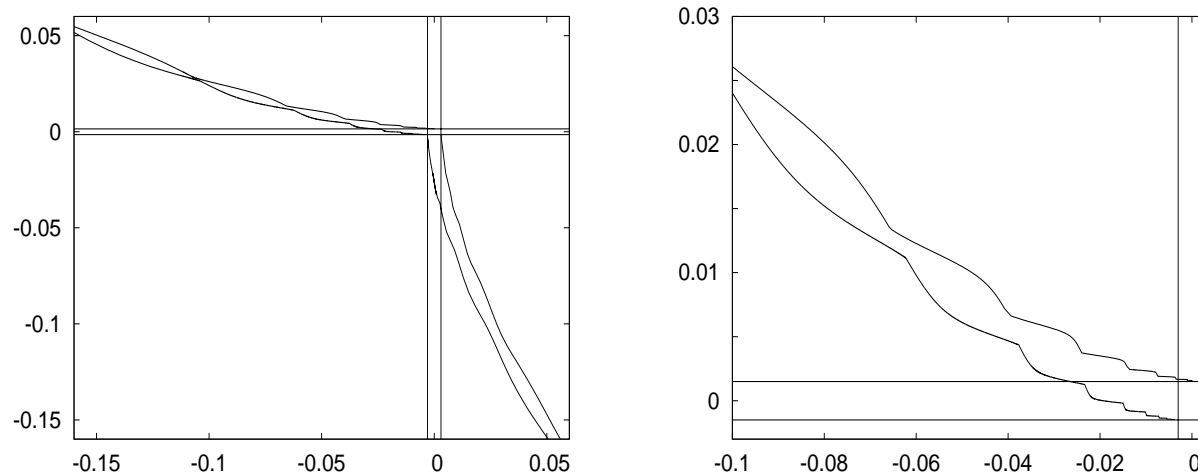
In the **simulations** we shall use $\omega_j = 0$, $A = 2$, $\psi = \lambda/\gamma = 1.6$.

Lemma: To recover qualitatively the flow case for $b_1 = b_2 = 0$ one requires $|a_j| < (\psi - 1)/\psi^{\psi/(\psi-1)}$, $j = 1, 2$.

b_1, b_2 are **perturbation parameters** set to $b_1 = 0.003, b_2 = 0.0015$.

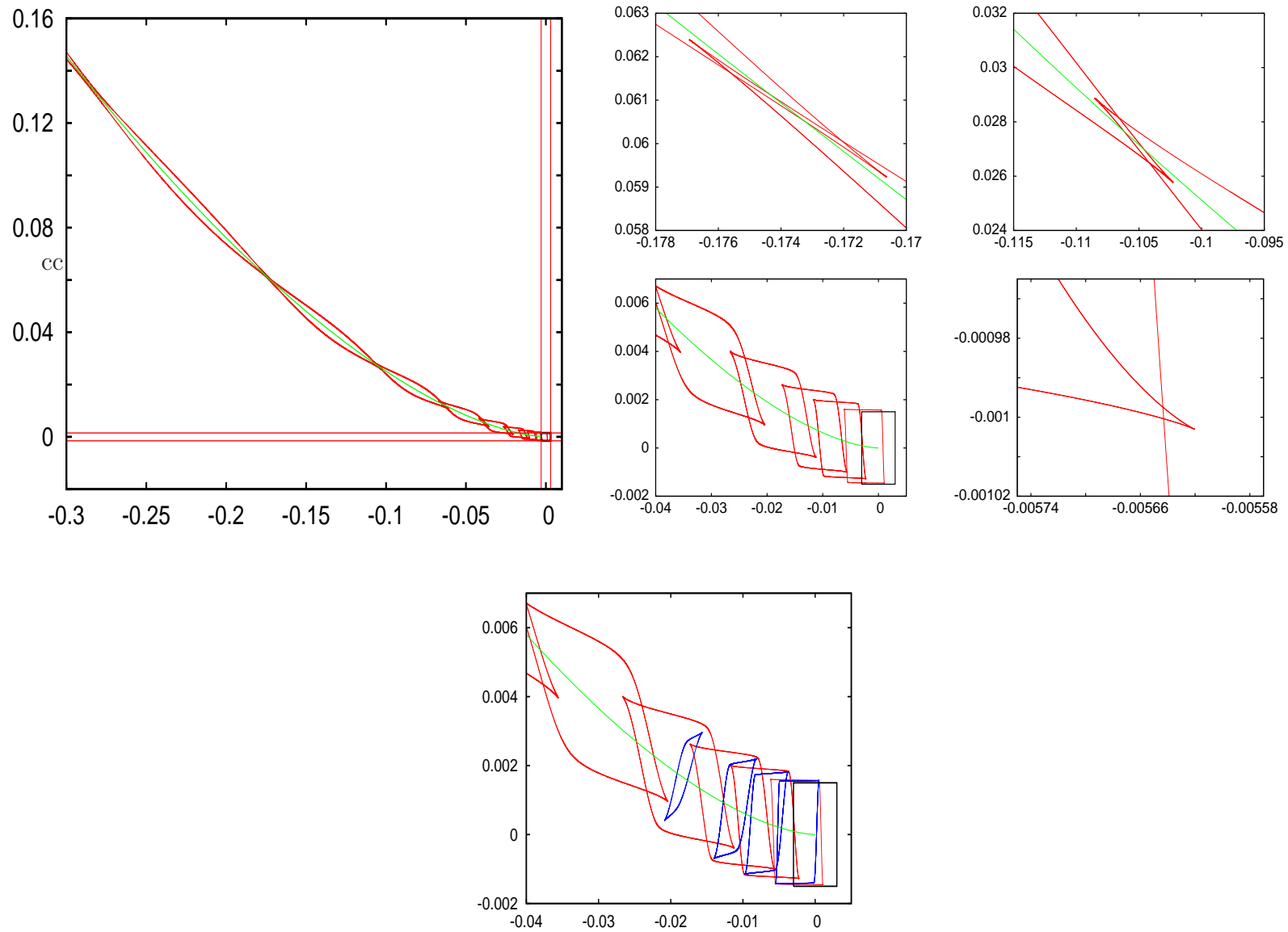
a_1, a_2 are taken as **leading parameters** ranging in $[-0.15, 0.15]$.

A preliminary exploration



Bifurcation curves corresponding to **first and last tangencies**. They bound different **homoclinic zones** in the parameter space (a_1, a_2) . Right plot is a detail of the boundary of the homoclinic zone HZ^\pm .

L_1^\pm , L_2^\pm , L_1^\mp and L_2^\mp are obtained by **joining different segments** of bifurcation curves corresponding to different **primary quadratic tangencies**. On next page we focus on the boundaries of HZ^\pm and some magnifications.

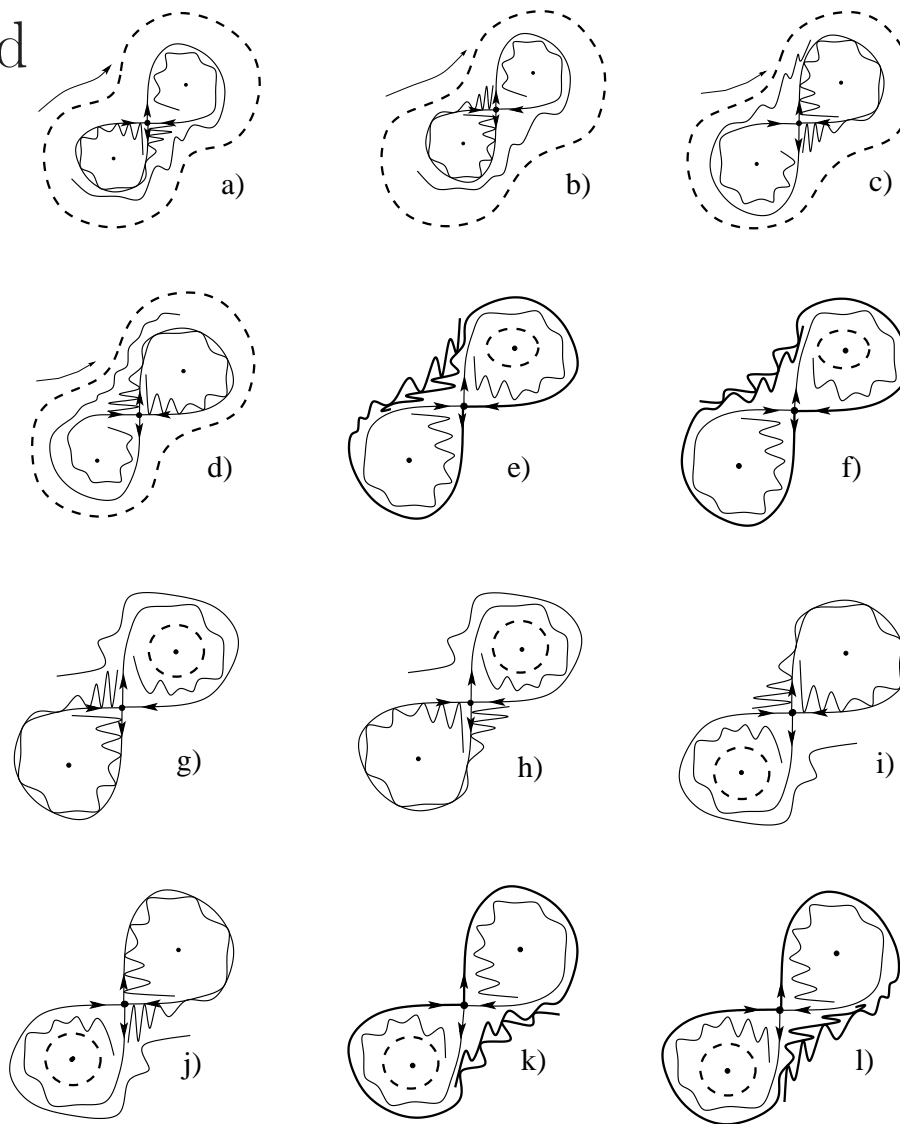


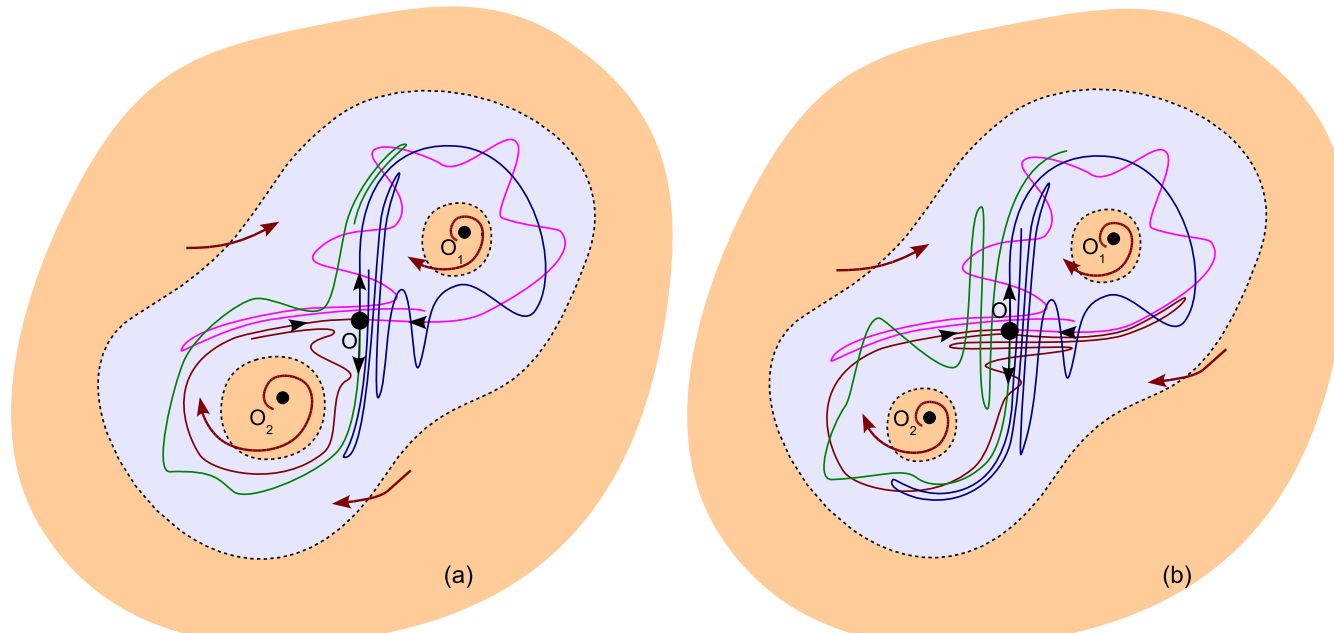
Quadratic tangencies and cusps. In red interlaced links accumulating to a and c . In blue curves which accumulate to b and d .

Kinds of tangencies and some homoclinic intersections

Homoclinic tangencies related to bifurcation curves.

- a) $\mu \in L_2^-, \mu_1 < 0$;
- b) $\mu \in L_1^-, \mu_1 < 0$;
- c) $\mu \in L_1^+, \mu_2 < 0$;
- d) $\mu \in L_2^+, \mu_1 < 0$;
- e) $\mu \in L_2^\mp$; f) $\mu \in L_1^\mp$;
- g) $\mu \in L_1^-, \mu_1 > 0$;
- h) $\mu \in L_2^-, \mu_1 > 0$;
- i) $\mu \in L_2^+, \mu_2 > 0$;
- j) $\mu \in L_1^+, \mu_2 > 0$;
- k) $\mu \in L_2^\pm$; l) $\mu \in L_1^\pm$.



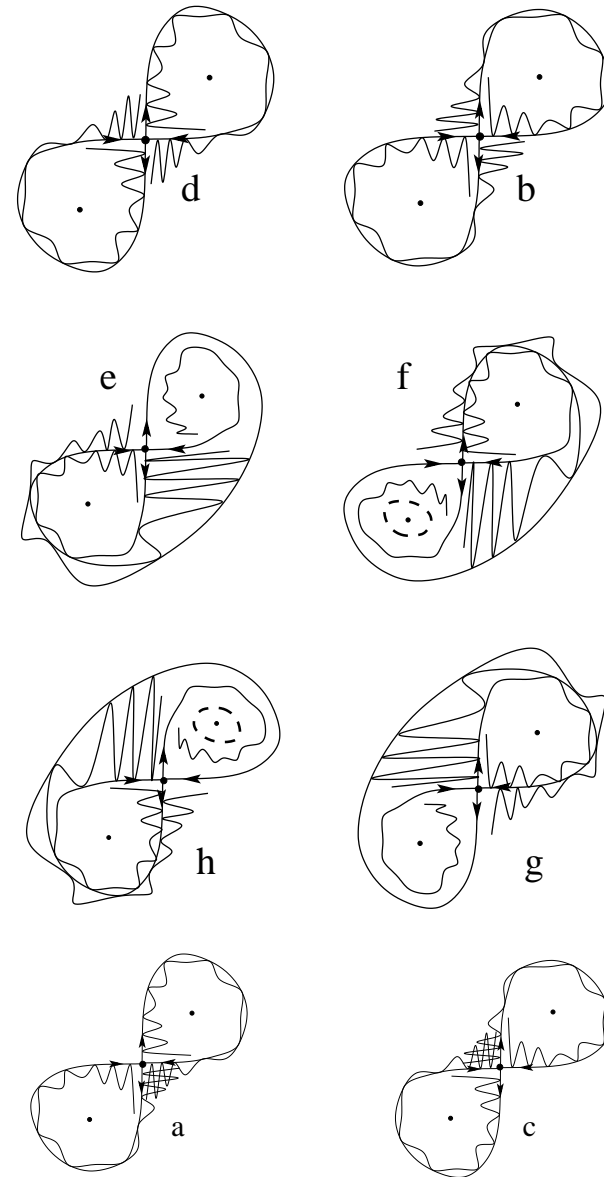


Homoclinic intersections:

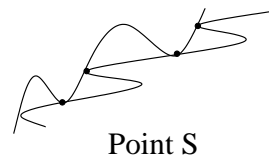
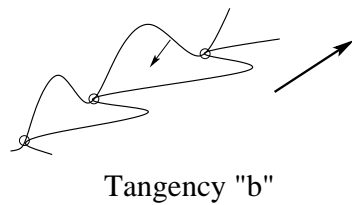
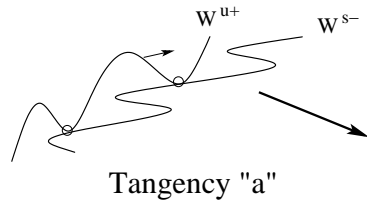
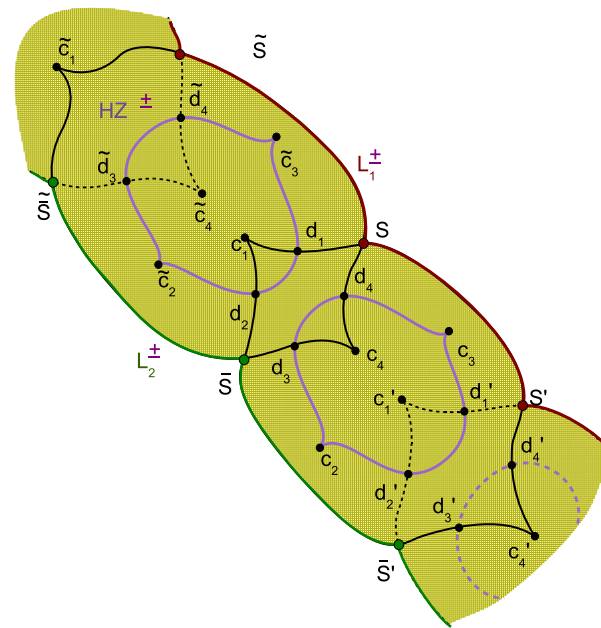
(a) in case $\mu \in \mathbf{26}$ in the bifurcation diagram. A “tail” strange attractor AT^+ exists.

(b) in case $\mu \in \mathbf{19}$ in the bifurcation diagram. A “global” strange attractor GA exists.

The boundaries of $HZ^{+, -, \pm, \mp}$ intersect at points of **double primary homoclinic tangencies** b, d, e, f, g, h and at **double not primary homoclinic tangencies** a, c .

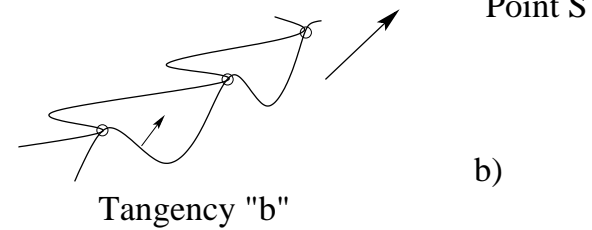
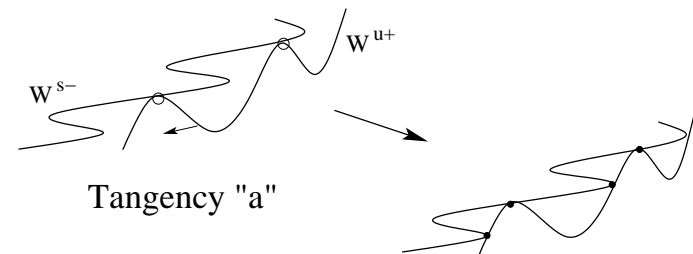


Bifurcation structure in the $HZ^{\pm, \mp}$ domains



a)

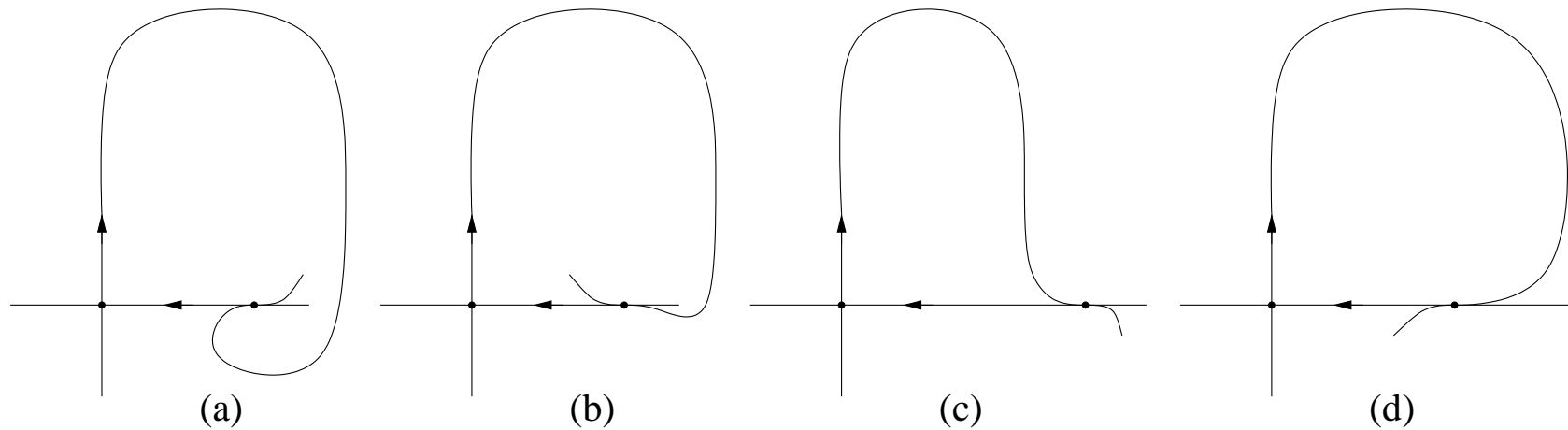
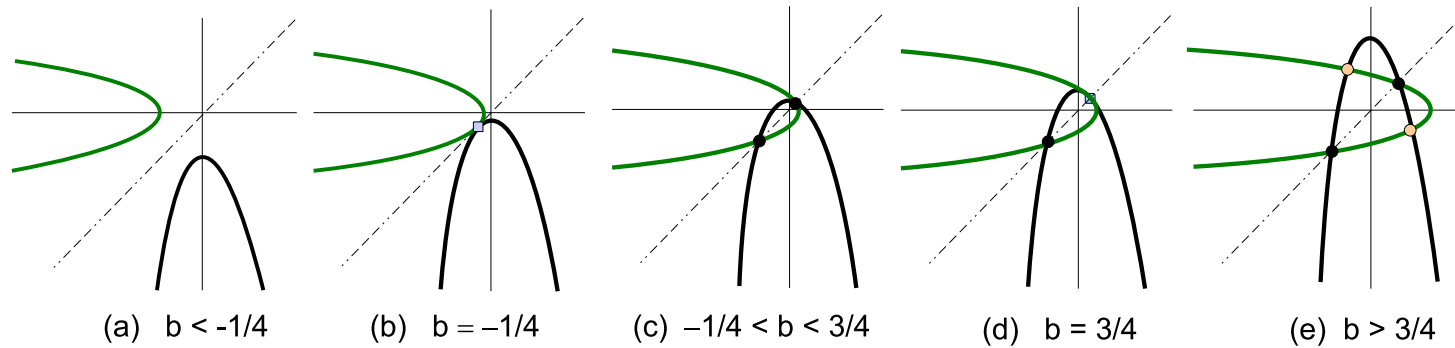
a) $\mu \in L_1^{\pm}$;



b)

b) $\mu \in L_1^{\mp}$.

Point \bar{S}



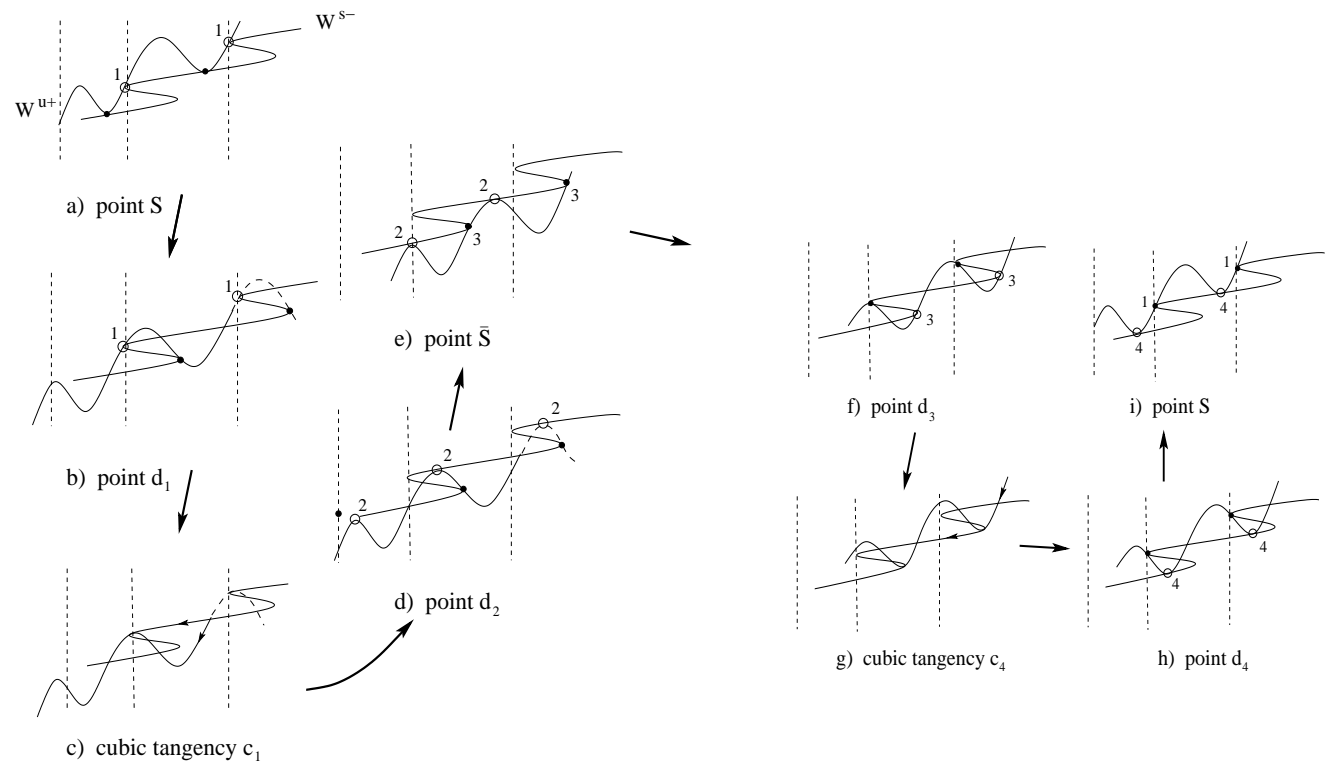
Top: creation of **cubic tangency** between parabolas.

Bottom: **primary cubic homoclinic tangencies**: (a) and (b) are of type “+” while (c) and (d) are of type “-”. The different type and other characteristics depend on **coefficients of the normal form** of the return map.

Sketch of **double quadratic** and **cubic** tangencies

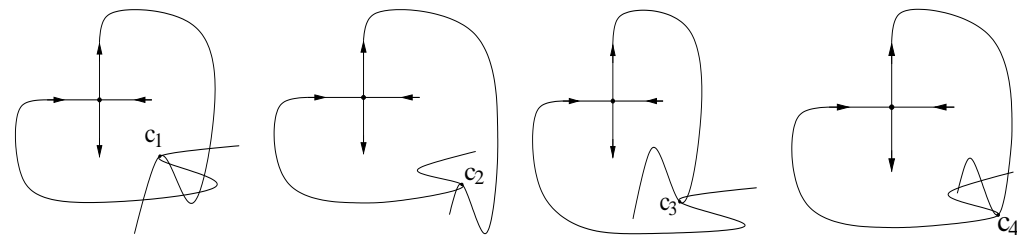
found following the path

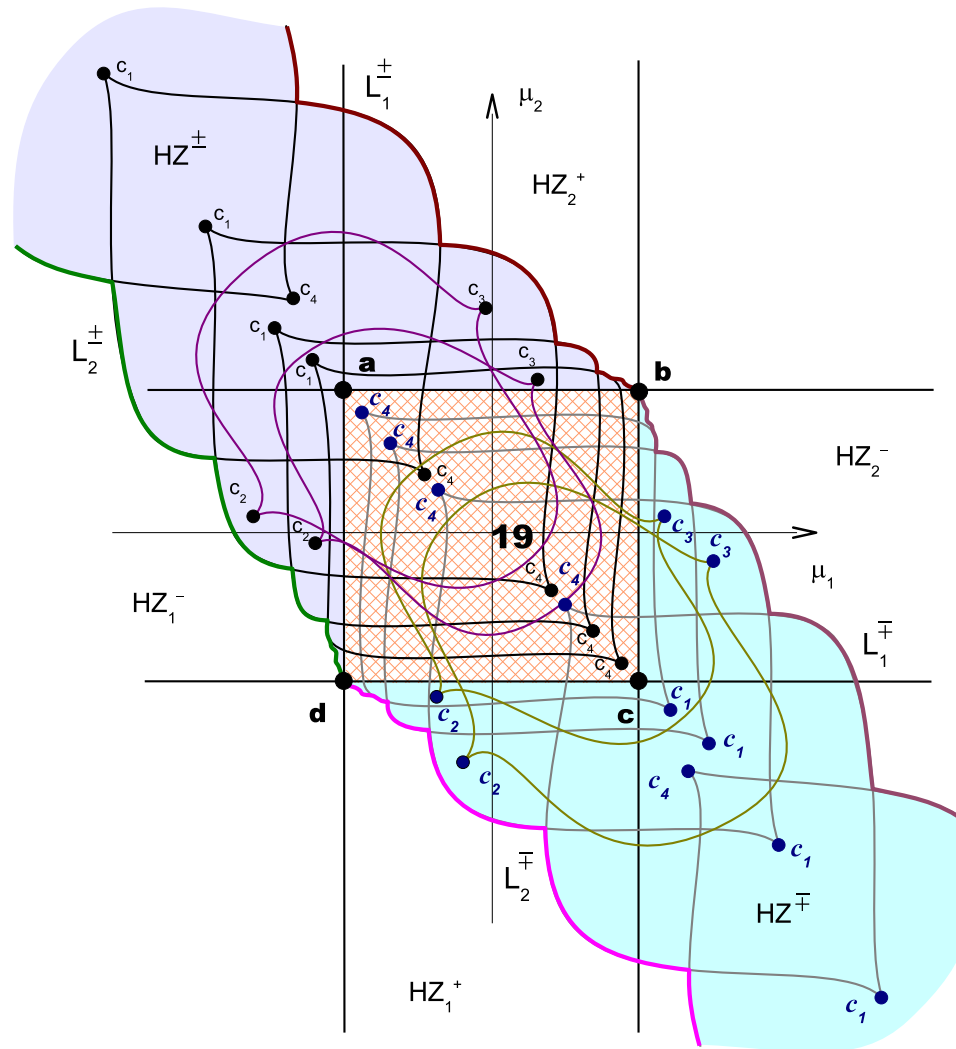
$$S \rightarrow c_1 \rightarrow \bar{S} \rightarrow c_4 \rightarrow S.$$



Primary homoclinic **cubic** tangencies

c_1, c_2, c_3, c_4
in HZ^\pm .





Accumulation of links to the square $abcd$.

Some theoretical results

Lemma. The primary homoclinic cubic tangency points (or the primary cusp points) c_1 , c_2 , c_3 and c_4 are of “-” type (i.e. spring-area). Concretely, c_1 and c_4 are topologically equivalent to the cubic tangency of type (d), while the c_2 and c_3 are top. equivalent to the cubic tangency of type (c). Concerning the rectangle $abcd$ of full intersection:

Lemma. The point b is the final point of the boundary curves L_1^\pm and L_1^\mp and d is the final point of the boundary curves L_2^\pm and L_2^\mp .

Lemma. For parameters $\mu \in \text{HZ}^\pm$ the following holds:

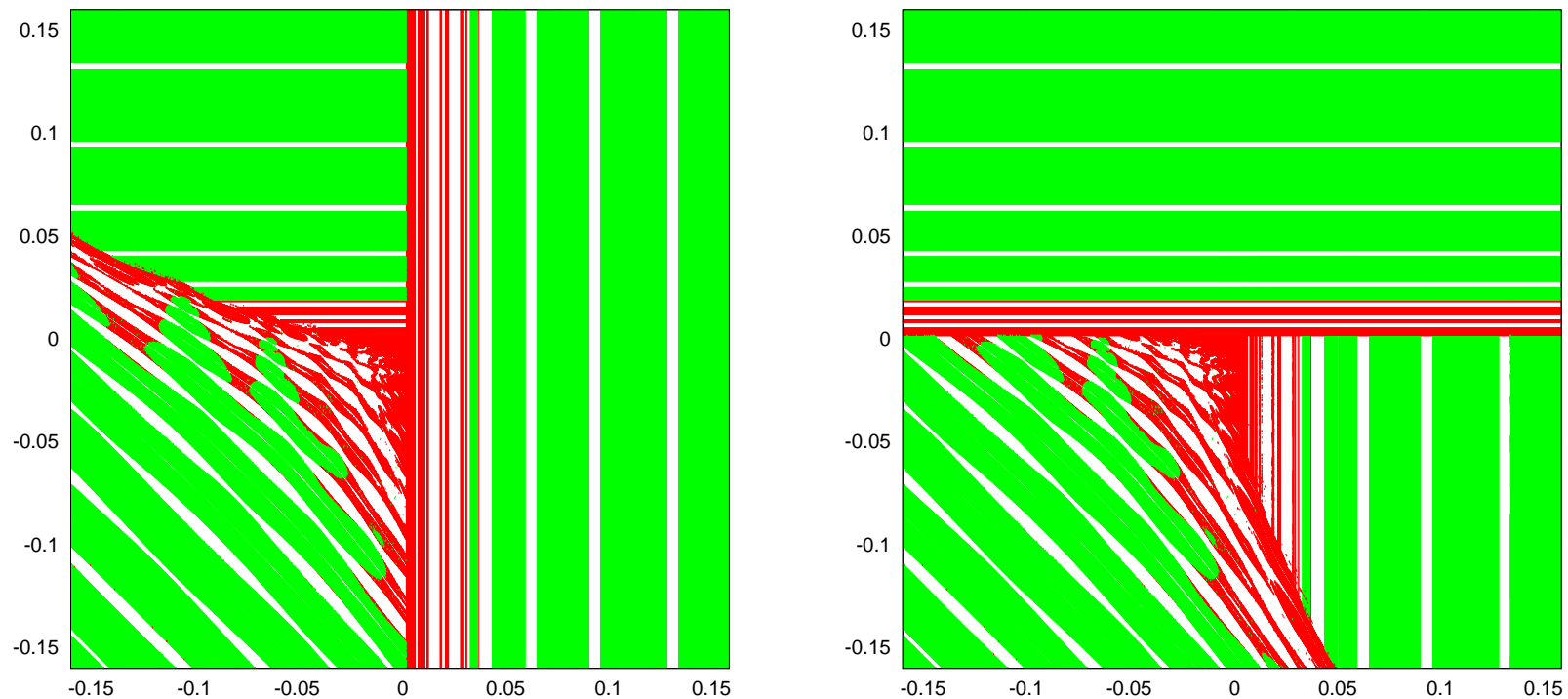
1. The primary cubic tangencies of type c_1 can exist only if $W^{u+} \cap W^{s+} = \emptyset$ and $W^{u-} \cap W^{s-} = \emptyset$. This means that c_1 can only exist in the regions **3** and **10** of the bifurcation diagram.
2. The primary cubic tangencies of type c_2 can exist if $W^{s+} \cap W^{u+} = \emptyset$. Thus, they can exist within the regions **3**, **10** and **18**.
3. The primary cubic tangencies of type c_3 can exist if $W^{s-} \cap W^{u-} = \emptyset$. Thus, they can exist within the regions **3**, **10** and **15**.
4. In the region **19** only primary cubic tangencies of type c_4 can exist.

Some corollaries follow.

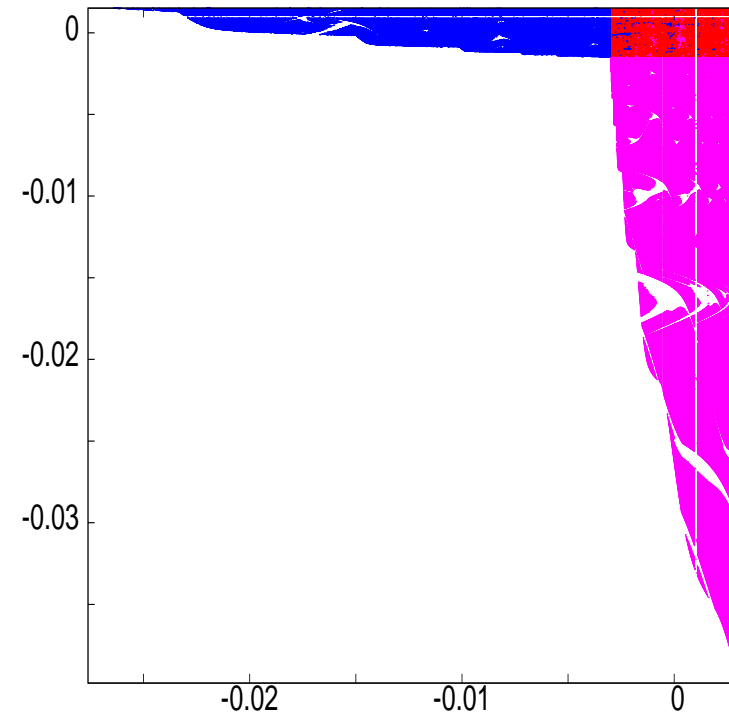
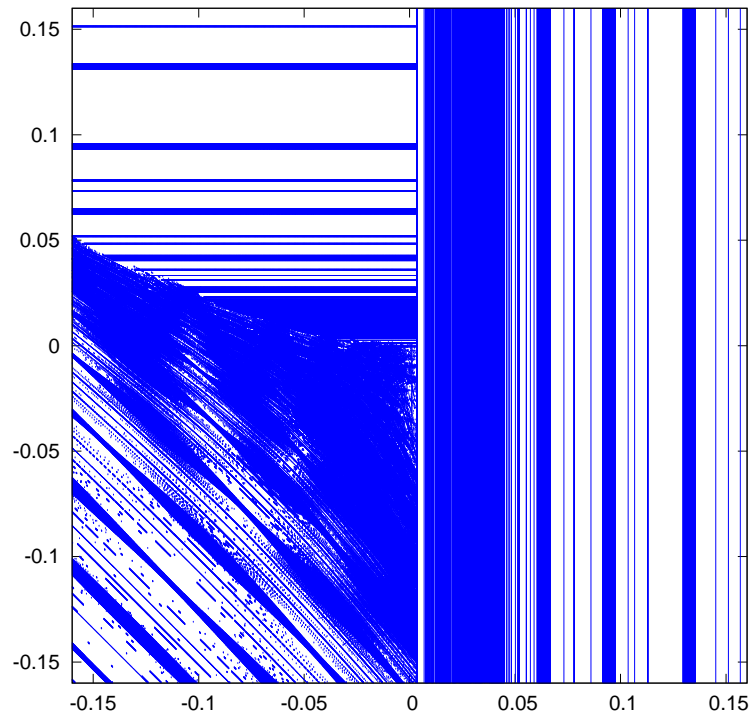
Corollary. The cusp points c_1, c_2, c_3 and c_4 accumulate to the points a, b, c and d respectively, which are the vertices of the rectangle bounding the zone GA.

Corollary. There exist infinitely many primary double quadratic tangencies corresponding to the intersection of the homoclinic branches related to the primary cubic tangency points of type c_1 and c_4 .

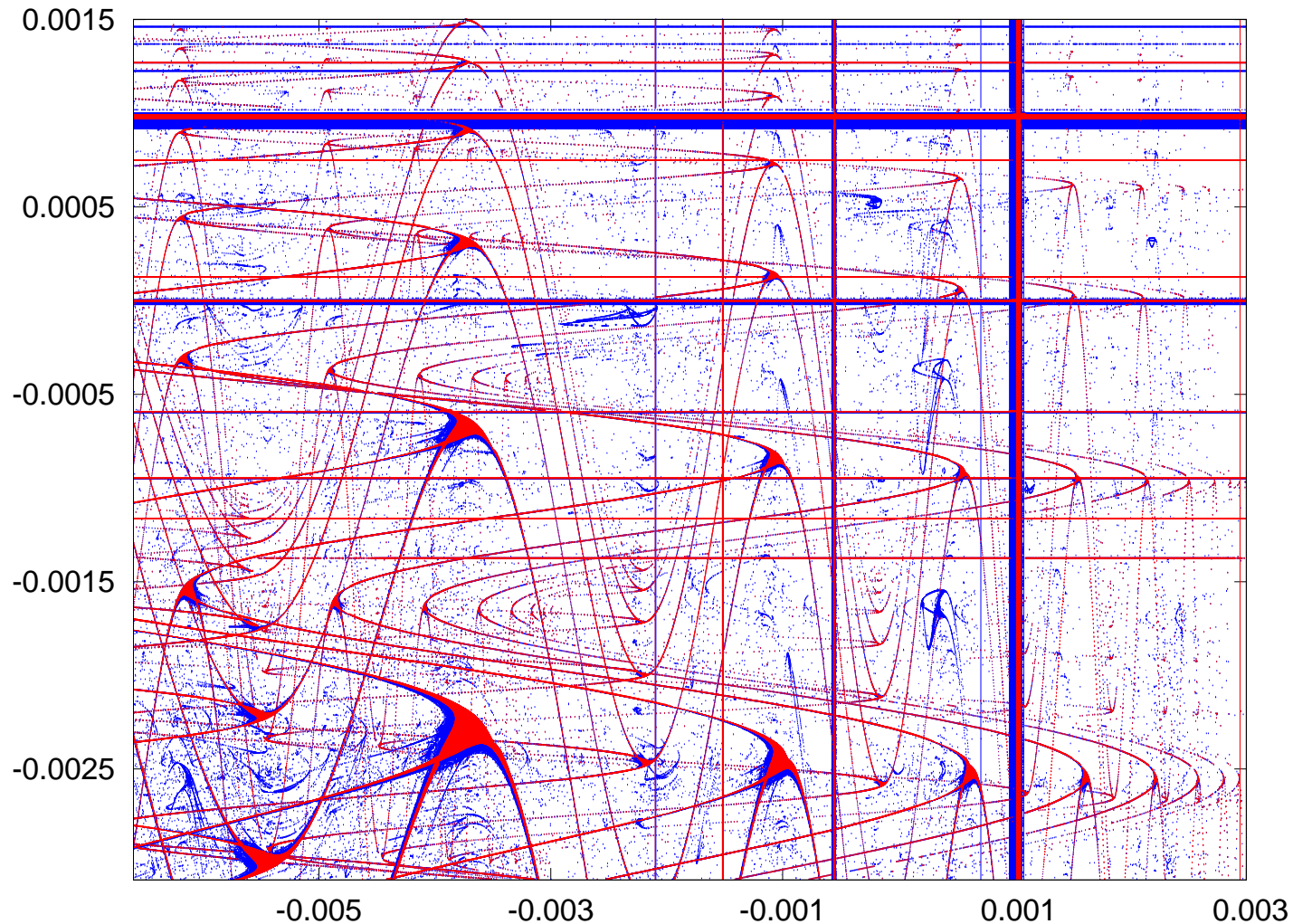
Further exploration of the model: global views



Maximal Lyapunov exponents (Λ) for the orbit with initial condition $(0.5, 0, s_0)$ with $s_0 = 1$ (**left**) and $s_0 = -1$ (**right**). **Red** points correspond to $\Lambda > 0$ (**chaotic attractor**), **green** points to $\Lambda = 0$ (**invariant curve**) and **white** points to $\Lambda < 0$ (**periodic sink**). Some white domains are **narrow** and can be seen by **magnifying**.

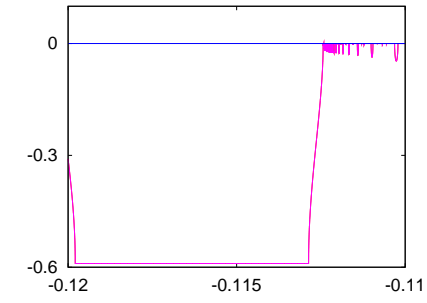
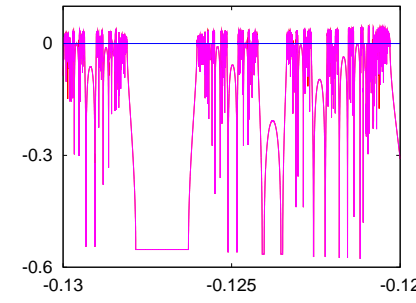
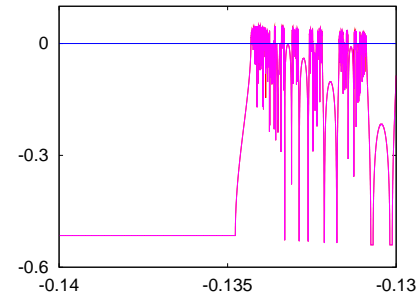
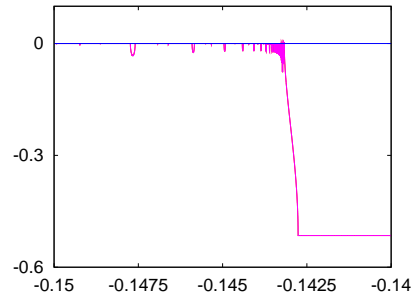
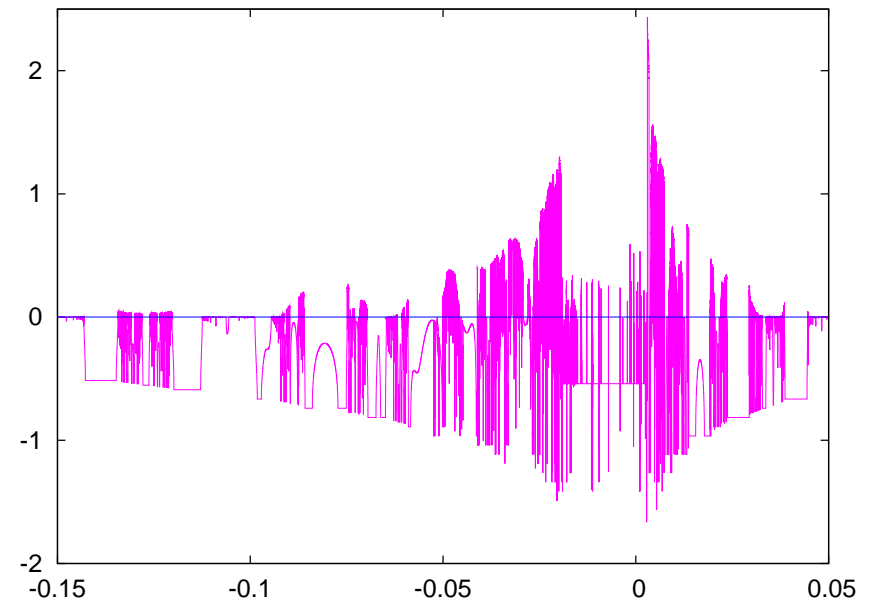
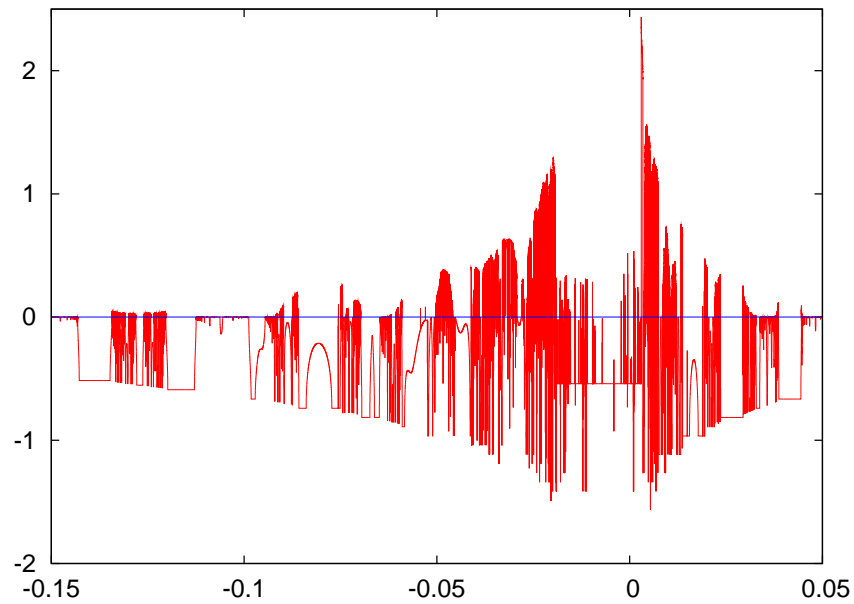


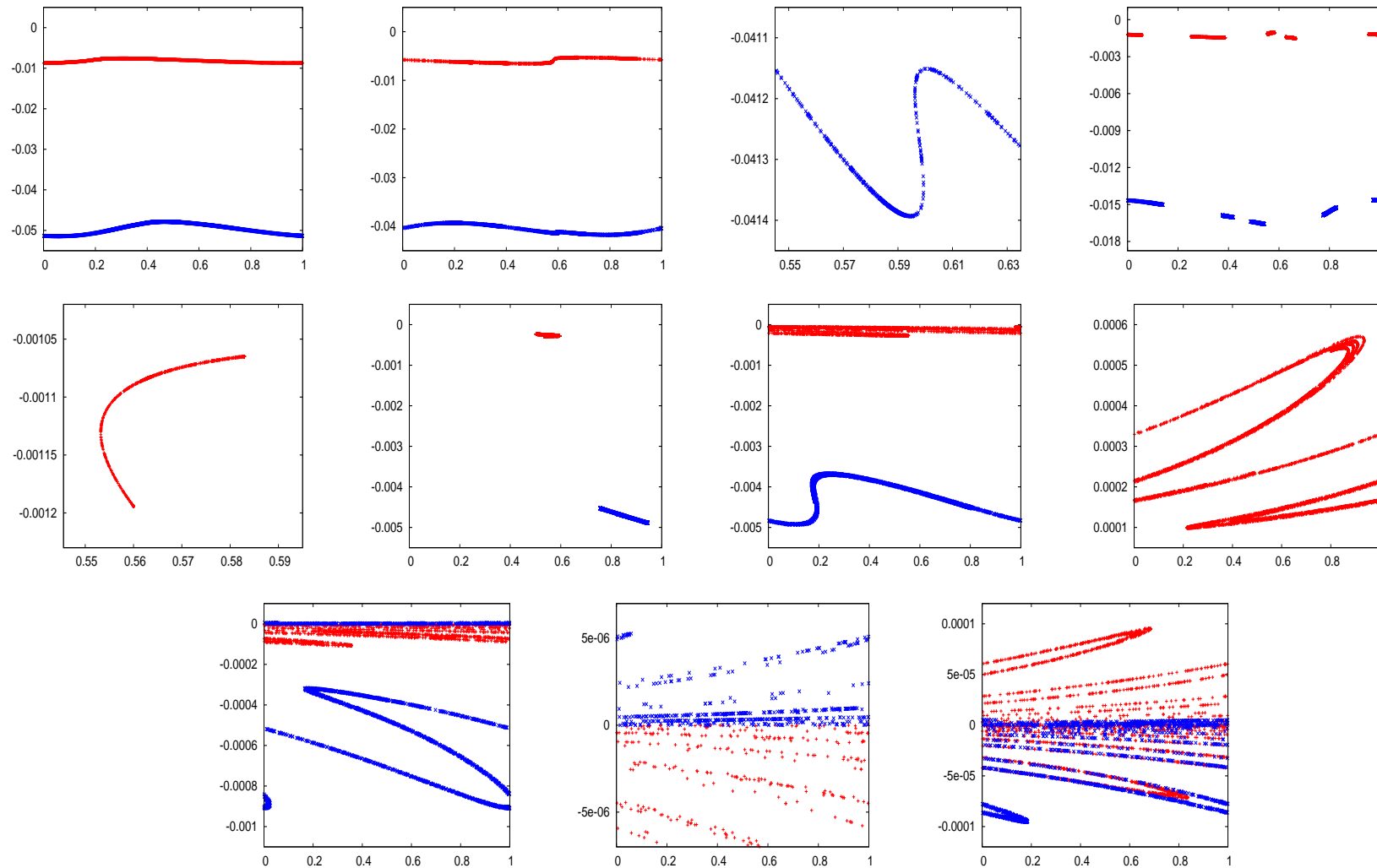
Left: Domains of **sinks**. Right: **Blue and magenta** are zones of **tail SA** AT^\pm . **Red** is a zone of **global SA** GA. Suggested: **magnify**.



In blue: set of (a_1, a_2) -parameters with computed $\Lambda < 0$ for the i.c. $(0.5, 0, 1)$. The attractor is a **periodic sink**. **In red:** parameters for which there is a **2-periodic sink** as attractor. Periods counted on the FD.

Domains of sinks, Lyapunov exponents, some attractors



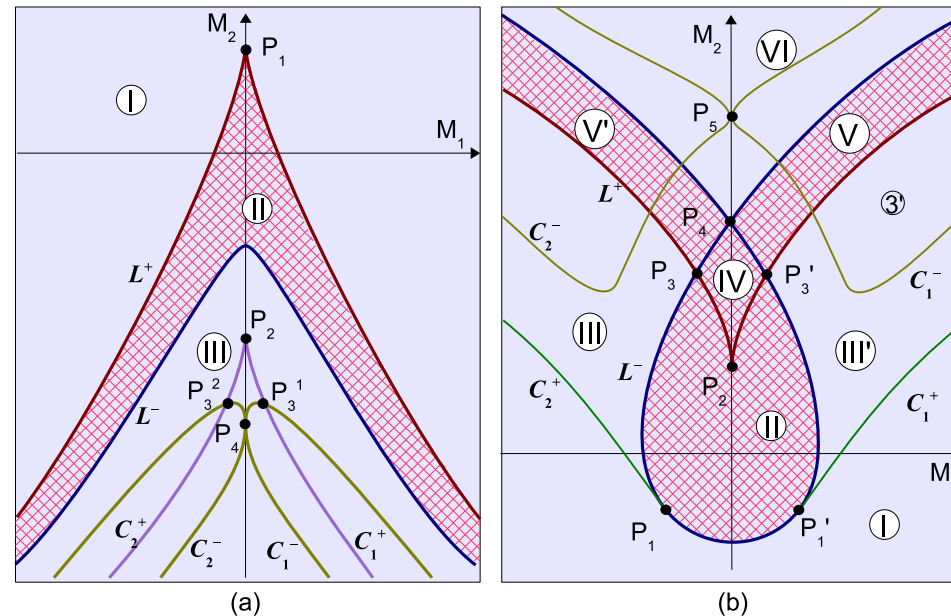


Top: A sample of attractors on $a_2 = 0$ for different values of a_1 . Bottom:
 Idem on $a_2 = -0.001$.

In **red**: points with $s = 1$. In **blue**: points in $s = -1$.

A sample of tools: cubic returns, sinks approaching a s-n

Suitable **expansions, normalizations and approximations** allow to derive a model for the **return near a cubic tangency**. The model is of the form $\bar{X} = Y, \bar{Y} = M_1 + M_2 Y + \beta_k X + \alpha Y^3$.



Left: **Saddle area**, $\alpha = 1$. Right: **Spring area**, $\alpha = -1$. **Codes:** L^+ fixed points with multiplier $+1$; L^- idem with -1 ; $C_{1,2}^+$ period 2 points with multiplier $+1$; $C_{1,2}^-$ idem with -1 (second period doubling).

There exist **cascades of sinks** which accumulate to the cubic tangency.

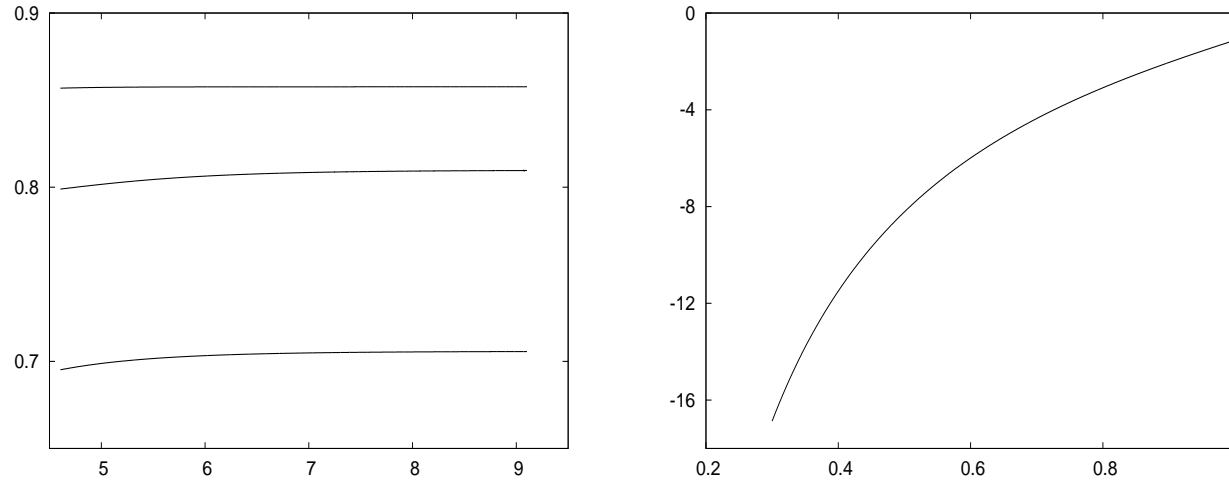
We consider the dynamics in an **inv. curve approaching a s-n**. Let F be an **analytic diffeomorphism in \mathbb{S}^1** as $x \mapsto x + a + bf(x)$ with $f(x) > 0 \forall x \in \mathbb{S}^1 \setminus \{0\}$, $f(0) = 0$, $df/dx(0) = 0$, $d^2f/dx^2(0) > 0$, $b \gg a > 0$.

For fixed b and a decreasing to 0 let $a_{sni}^{(k)}$ be the **beginning of existence of sinks** of period k and $a_{snf}^{(k)}$ be the **final**.

Proposition. Then, generically,

1. $a_{sni}^{(k)}$ and $a_{snf}^{(k)}$ behave as $c_1/k^2 + \mathcal{O}(1/k^3)$.
2. $(a_{sni}^{(k)} - a_{snf}^{(k)}) / (a_{sni}^{(k)} - a_{sni}^{(k+1)})$ has a limit depending on b .
3. the minimal multiplier in $[a_{snf}^{(k)}, a_{sni}^{(k)}]$ has limit < 1 , depending on b .

As an example consider the **Arnold map** with $f(x) = 1 - \cos(x)$.



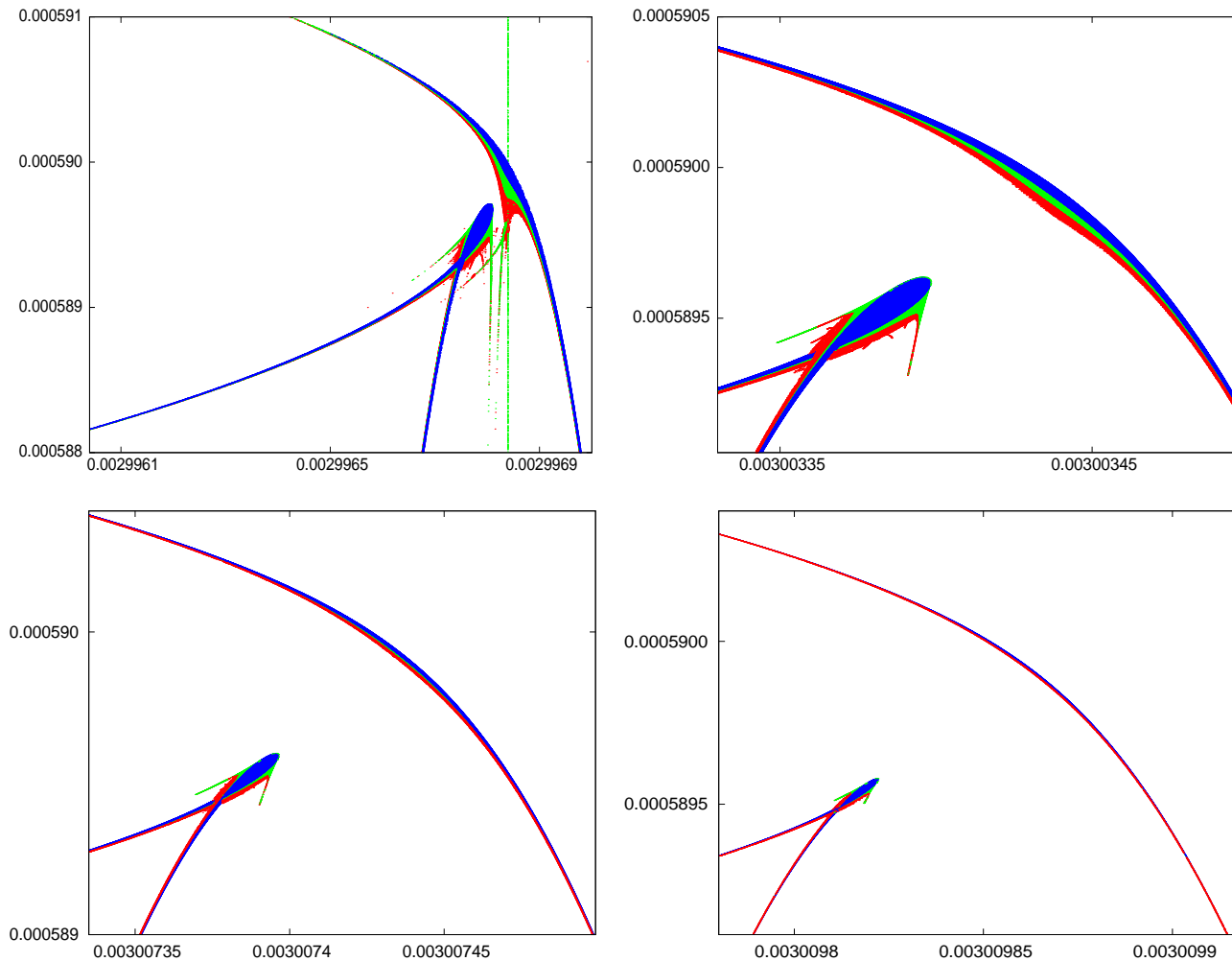
Left: Plots as a **function of $\log(k)$** from bottom to top of:

1) $\log(a_{snm}^{(k)}) + 2 \log(k) - 2.5$; 2) $\log(\Delta a_{sn}^{(k)}) + 3 \log(k)$; 3) the multiplier for $a \in [a_{snf}^{(k)}, a_{sni}^{(k)}]$ at which it reaches a minimum.

$$a_{snm}^{(k)} = (a_{sni}^{(k)} + a_{snf}^{(k)})/2; \Delta a_{sn}^{(k)} = a_{sni}^{(k)} - a_{snf}^{(k)}.$$

Right: The function $\Delta g(b)$ which **measures the limit in 2)** as a **function of b** . Plotted: $\log(\Delta g)$ versus b . Note the **exponentially small** character of Δg .

An illustration of blowing up near the limit



Note the progressive **destruction of a previous cross-road** domain.

Outlook: open problems and extensions

Several questions remain **open**, like

- The **creation/destruction** of SA by **folding** of IC.
- In particular the **boundary green-red** domains in the model, **marked as BD** in the bifurcation diagram.
- The **abundance** of sinks, taking into account the existence of **cross-road and spring** areas.
- **Links with s-n boundaries** connecting different cross-road and spring areas.
- Relative **size** of the **basins of attraction** when there is **multiplicity of attractors**.

And possible **extensions** to **3D and higher dimension** diffeomorphisms. E.g.: Shilnikov-like, Hopf-Shilnikov-like maps, etc.